

1 **Assessment of thermophysical properties of hybrid nanoparticles (Graphene nanoplatelets**
2 **(GNPs) and Cellulose nanocrystal (CNC)) in a base fluid for heat transfer applications**

3

4 M. Sandhya ^{a, b, *}, D. Ramasamy ^{a, b}, K. Kadirgama ^{b, c, d}, W.S.W. Harun ^a, R. Saidur ^{e, f}

5 ^a College of Engineering, University Malaysia Pahang, 26300 Gambang, Pahang, Malaysia

6 ^b Advanced Nano Coolant-Lubricant (ANCL), College of Engineering, Universiti Malaysia
7 Pahang, 26600 Pekan, Pahang, Malaysia

8 ^c Faculty of Mechanical and Automotive Engineering Technology, Universiti Malaysia Pahang,
9 26600 Pekan, Pahang, Malaysia

10 ^d Automotive Engineering Centre, Universiti Malaysia Pahang, 26600 Pekan, Malaysia

11 ^e Research Centre for Nano-Materials and Energy Technology (RCNMET), School of Science and
12 Technology, Sunway University, Malaysia

13 ^f Department of Engineering, Lancaster University, Lancaster, LA1 4YW, UK

14 *Corresponding author E-mail: madderla.sandhya@gmail.com (Madderla Sandhya)

15

16 **Abstract**

17 This article comprehensively investigates single (GNP) and hybrid nanofluids (GNP/CNC
18 nanoparticles), including nanofluid preparation and thermophysical properties. Nanoparticles were
19 characterized using FESEM and XRD analyses. A two-step approach for the preparation of
20 nanofluids was employed, and the prepared nanofluids were determined by various analytical

21 techniques. The thermal conductivity of nanofluids was measured in the range of 20–50 °C of the
22 temperature using the ASTM D2717–95 norm, and the volume concentration range of the Nano-
23 fluid in this research ranged from 0.01-0.2%. For the single GNP nanofluid, temperatures at room
24 level indicated the thermal conductivity value in the range of 0.366-0.441 W/m-K, and for hybrid
25 nanofluid, the thermal conductivity values are in the range of 0.501-0.551 W/m-K. In addition, the
26 viscosity, density, and specific heat of the nanofluids are also measured and discussed. The
27 theoretical and experimental density values come in pact with a minor error percentage increasing
28 with the concentration of nanoparticles with a value of 1050 kg/m³ & 1060 kg/m³ for 0.01 %
29 concentration of mono/hybrid nanofluids, respectively. Finally, based on the findings, it can be
30 determined that the thermal conductivity properties of the selected nanoparticles are beneficial,
31 and hybrid Nano-fluid is an acceptable alternative to conventional/water-based fluids in terms of
32 thermal properties in operational systems.

33 **Keywords:** Thermal conductivity, viscosity, Graphene nanoplatelets, crystal nanocellulose,
34 Hybrids

35 **1. Introduction**

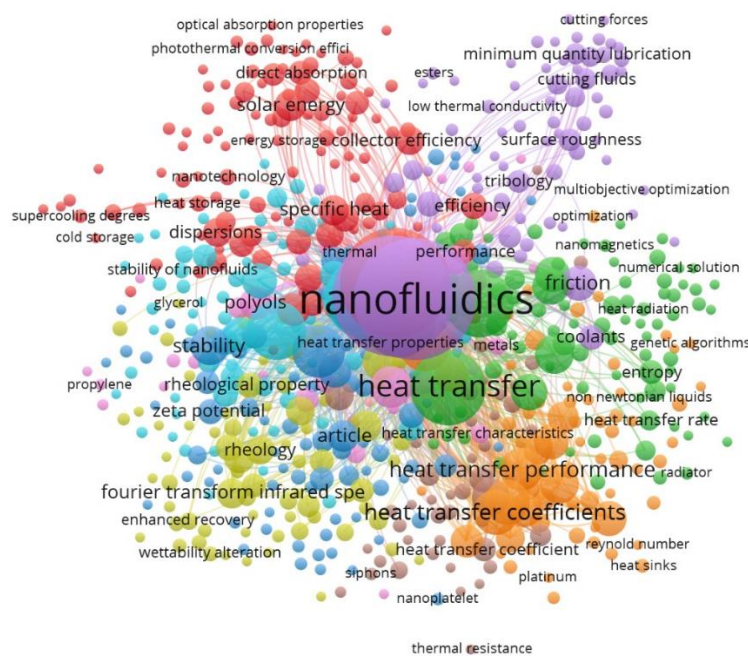
36 The utilization of solid nanoscale particles distributed in the base fluid is a groundbreaking
37 approach for enhancing the thermal functioning of heat transfer solutions. Nanofluids in this
38 research were produced as a modern heat transfer solution by combining solid nanometer sized
39 particles of graphene nanoplatelets/cellulose nano crystals at minimal concentrations with the base
40 fluid (ethylene glycol: water; 60:40). Heat transfer is a concern of practical significance and
41 prominence in the industries [1]. The potential of fluids to heat flow performs a significant
42 responsibility in the quantity of heat loss and, in general, thermal conduction. Many industries rely
43 on water, ethylene glycol, and oil [2, 3] kind of fluids. Considering current innovations and new

44 technologies in certain sectors, it is important to enhance the efficiency of this type of fluids'
45 thermal properties and ability to use them. Researchers are currently experimenting with Nano-
46 fluids and ensuring appropriate stabilization of Nanoparticles in base fluids to enhance their
47 heat properties [4].

48 Nanoparticles are distributed in a “traditional” operating fluid such as water or the anti-freeze
49 ethylene glycol to create a efficient substitute working fluid for enhanced heat transfer called
50 “nanofluid” [5]. Choi and Eastman [6] first proposed the term "nano-fluid" in 1995, referring to
51 the presence of nanoparticles with diameters of 1–100 nm in base fluids. Investigators have
52 discovered that application to a working fluid by introducing nanoparticles change its
53 thermophysical properties dramatically in the new decade [7]. The certainly changed thermal
54 properties of the dispersed nanoparticles in the base fluid in evaluation to the traditional fluid have
55 resulted in some noteworthy improvements in the nanofluids thermal properties [8], such as
56 thermal conductivity and convective efficiency of the heat transfer(CHT). Metal oxide
57 nanoparticles, such as Al_2O_3 , CuO, ZnO, and TiO_2 , or carbon-based particles, such as carbon
58 nanotubes (CNTs), graphene oxide (GO), and graphene nanoplatelets (GNPs), are examples of
59 nanoparticles [9]. Since single/multi-wall carbon nanotubes, graphite, graphene/graphene oxide
60 are carbon-based nanoparticles, are sometimes referred to as miraculous nanoparticles, many
61 scientists are currently focusing on them to develop nanofluids with large-aspect-ratio
62 nanoparticles with improved thermal, mechanical, and catalytic characteristics [10]. As all
63 nanoparticles with carbon-base have a superior thermal conductivity, and these nanofluids have
64 significantly enhanced thermal properties like thermal conductivity including coefficients of heat
65 transfer. For improving heat transfer coefficient and thermal conductivity of heat exchanging fluid,
66 the majority of preliminary research has been conducted on single/mono nanoparticles for the

67 reason that of its unusual physical properties or thermal properties and mechanical or electrical
68 properties [11, 12]. Graphene has fascinated a lot of consideration as a two-dimensional of carbon
69 atoms with single layer [13]. Graphene nanoplatelets, on the other hand, (which are made up of
70 numerous layers of graphene) bring the advantages together of monolayer property, such as the
71 area of surface a high and great thermal conductivity, alongside of tightly packed graphitic carbon
72 advantages, also such as strong stable nature and low budget. Due of strong Van der Waals
73 interactions, GNPs, on the other hand, be likely to accumulate between the cause of large specific
74 surface area [14, 15]. Below figure 1 show the important properties related to nanofluids for the
75 thermal application obtained from the Scopus data.

76



77

78 Figure 1 Bibliographic representation of accomplished properties related to nanofluids

79 “Nanocomposite” refers to the synthesis of at least two distinct nanoparticles into one. Sundar,
80 Singh [16] produced MWCNT-Fe₃O₄ nanocomposite and developed a hybrid nanofluid, achieving
81 a 29 percent increase in thermal conductivity at 0.3 percent concentration by volume in water at
82 60 °C. Theres Baby and Sundara [17] developed a hybrid nanofluid and observed an increase of
83 8% in thermal conductivity for Ag/MWCNT-HEG at a volume fraction of 0.04 percent and at 25
84 °C. Amiri, Shanbedi [18] studied the properties in rheological terms of MWCNT–Ag
85 nanocomposite using both covalent and noncovalent polymerization methods and discovered that
86 the covalent method is better for sustained thermophysical properties of nanofluid. As the
87 Graphene nanoplatelets are hydrophobic in nature [19], the functionalization process which used
88 to generate suspension of stable nanofluids with graphene is appropriate for nanofluids
89 applications. With a yearly output of approximately 7.6x10¹⁰ ton, cellulose is the most abundant
90 renewable organic substance [20]. Nanosized cellulose have recently attracted attention due to
91 their extraordinary high specific strength and modulus, low density, chemical adaptability,
92 renewable "green" nature, and affordable cost [21]. Few of the research has been made on finding
93 the mechanical properties of the prepared hybrid nanocellulose fluid but there is no or limited
94 research on hybrid cellulose for thermophysical properties for thermal application [22, 23].
95 Cellulose nanocrystals (CNC) are fibrillar form, with a diameter of about 5 nm and a length that
96 varies depending on their source and fabrication process [24]. cellulose, the most common organic
97 substance as from ecosystem, is renewable, biodegradable, biocompatibility, non-toxic, and
98 environmentally friendly attributable to its recyclability, biodegradability, cytocompatibility, and
99 environmental friendliness [25], has drawn increasing attention in several disciplines and could
100 serve as a notable alternative to thermal applications. The benefits of cellulose can also be
101 advanced by investigating its nonmetric size, which results in nanocellulose, which is regarded as

102 a capable class of forthcoming materials expected to its remarkable physicochemical capabilities.
103 Nano cellulose has a low density, dilatation morphology, inertness, wide surface area and aspect
104 ratio, and is abundant and easy to bio-conjugate. Due of their unique physicochemical, mechanical,
105 thermal, rheological, and optical properties, CNC-based nanomaterials have been widely studied.
106 CNC could provide acceptable features to hybridization or nanocomposites (metallic, ceramics,
107 and polymeric) however at low concentrations for a wide range of applications. Fullerenes, carbon
108 nanotube (single-walled, double-walled, few-walled, or multi-walled), nano diamonds, as well as
109 graphene-based materials like graphene, oxide form of graphene, reduced form of graphene oxide,
110 and graphene quantum dots have evolved into a new category of hybrid materials with a synergetic
111 effect or synergetic effect in a variety of applications. Despite the fact that several potentially
112 possible techniques to produce effective Graphene nanoplatelets are now being developed, there
113 are still several practical difficulties to overcome. GNPs, for example, are further normally
114 generated from aqueous dispersals, although they can effortlessly agglomerate. This type of
115 agglomeration can limit surface area and have a detrimental impact on properties. As a result, the
116 addition of CNC not only overcomes this disadvantage due to its exceptional disseminative
117 properties, but similarly converses additional assistances to the resulting GNP/CNC hybrids, such
118 as quick dispersion and thermal stability, as well as improved adsorption capability, photothermal
119 interaction, sustainability, intrinsic luminosity and diffraction, optical transparency, and thermal
120 conductivity. Considering these facts, it is clear that using CNC as a companion material in GNP
121 nanoparticles could be more effective and beneficial in improving the nanocomposite's thermal
122 conductivity as well as thermal properties. We detail the preparation, and thermal properties of
123 GNPs/CNC hybrid fluids in this study. This paper presents a forward-considering perspective on
124 GNPs/CNC hybrids for a variety of applications. Nonetheless, the progression of

125 GNPCNC hybrid-based nanomaterials is a comparatively innovative belief that is largely
126 restricted to scholarly disciplines. However, it is expected that several hybrid nanofluids (graphene
127 based) research will become more attractive in the potential, attracting more study consideration
128 not only in several functions but additionally in achieving multifunctional systems and opening
129 new perceptions. Furthermore, the sensible implementation of such hybrids as next-group
130 materials necessitates significant functional and performance enhancements. The present study
131 focuses on the comparison of nanofluids thermophysical properties with single and hybrid
132 Graphene based nanofluid. As there is no data available in the literature for the novel work as this
133 kind on the thermophysical properties assessment of hybrid nanoparticles including the Graphene
134 nanoplatelets and cellulose nano crystals in a base fluid of ethylene glycol and water at a ratio of
135 60:40.

136

137 **2. Methodology**

138 This research process offers comprehensive details about the analysis, the materials as well as
139 equipment utilized for the characterization of nanofluids (Water & Ethylene glycol -based GNPs /
140 CNC), nanoparticles of Single/ Hybrid and accompanied by an examination on stability.

141

142 **2.1 Materials**

143 In this investigation, graphene nanoplatelets (GNPs) with 800 m²/g specific surface area
144 (S.A) were employed, which were purchased from Nanografi nanotechnology (USA) with 99.9%
145 purity, 3nm Size, and 1.5 μm in diameter, and crystalline nanocellulose from the country Malaysia
146 by MY Biomass Sdn. Bhd. CNC remained challenging to separate in powder type from the

147 produced pulp because of its hydrophilic character. A spray-drying approach with a tiny fan was
148 employed for CNC handling in the form of powder. When the pulp or suspensions reached into
149 connection with heated air from the nozzle spray dryer's entering space, the moisture quickly
150 evaporated, resulting in steady CNCs flake. The flakes of CNC are collected and ground into
151 powder. The specific parameters of the obtained CNC nanoparticles crystallinity index with 80%,
152 100-150nm crystal length, 9-14nm crystals diameter, and the hydrodynamic diameter is 150nm.

153 2.2 Preparation of nanofluid

154 At a concentration by volume as 0.01%, 0.05%, 0.1%, & 0.2%, the graphene nanoplatelets are
155 weighed by means of the Internal Sartorius Analytical Balance (Model : BSA24S-CW) and were
156 scattered in the Ethylene glycol-distilled water which is at a ratio of 60:40 by using a magnetic
157 stirrer with rotating magnetic probe (Thermo-fisher, USA) and is was allowed to stir for about 2
158 hours and later the probe of the ultrasonication (CE ISO Ultrasonic Homogenizer Sonicator
159 Processor Cell Disruptor Mixer 20-1000mL) having an productivity control over power of 950 W
160 and a frequency choice as 20kHz supply of power with a ϕ 13mm diameter probe. By using Eq
161 (1), the density of hybrid nanoparticles is calculated.

$$162 \quad \rho_{\text{GNP/CNC}} = \frac{\phi_{\text{GNP}}\rho_{\text{GNP}} + \phi_{\text{CNC}}\rho_{\text{CNC}}}{\phi_{\text{total}}} \quad (1)$$

163

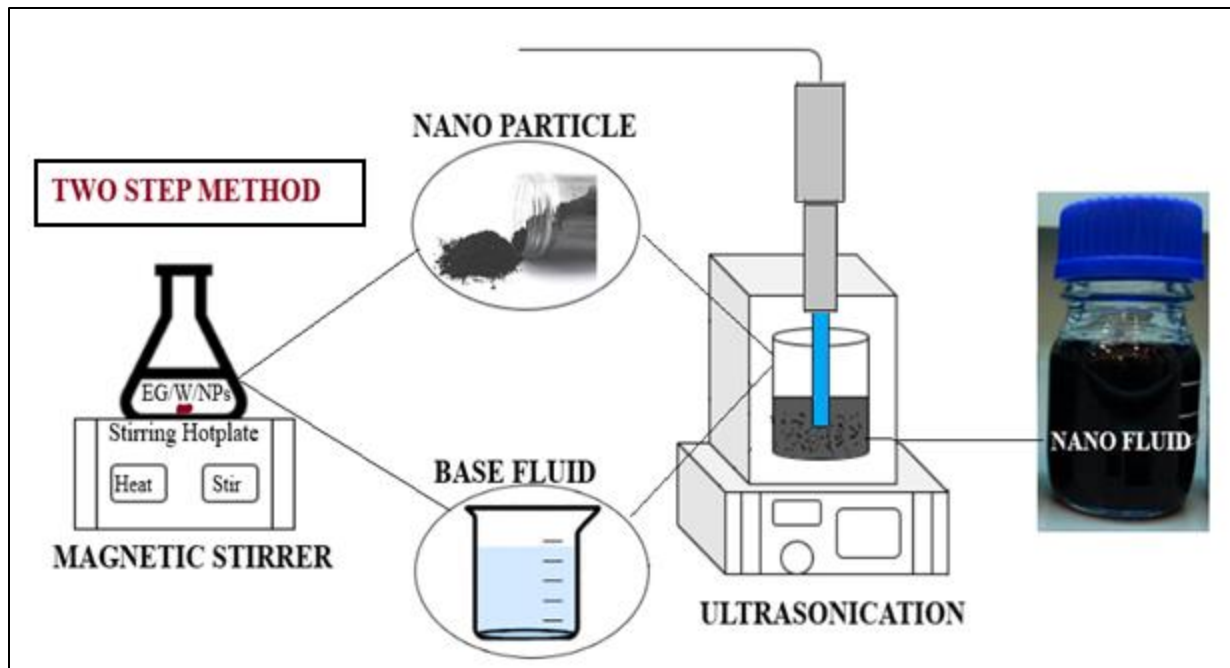
164 Where, GNP denoted Graphene Nano Platelets, CNC denote Cellulose Nano Crystal, ' ϕ ' denotes
165 the volume concentration of nanoparticles in nanofluids and ' ρ ' denotes density respectively.

166

167 In the absence of a surfactant, since nanoparticles of carbon-based having a hydrophobic nature,
168 they cannot be sustainably distributed in base fluid. Graphene nanoplatelets, as a result of their
169 electrical and thermal conduction, are graphite form. The GNPs are recommended that they can
170 be scattered in medium with stirrer & sonication through a probe without utilizing surfactants.
171 Therefore, 5 hours of ultrasonication time was used to make the particles properly disperse and
172 stable with a power utilization of 50%. Likewise, preparation of hybrid nanofluid contains the
173 particles GNPs / CNCs at 1:1 ratio is disseminated in the base fluid Ethylene Glycol-distilled water
174 (60:40) with a magnetic stirrer (Thermo-fisher, USA). This high-speed stirrer operated at a range
175 of 400-500 rpm until proper blending/mixing for about 120-180 minutes and altered for every 15
176 mins followed by ultrasonication procedure with a probe for 5 hours with a power output of 50%
177 with interval gap of 5 mins after every 15 minutes of sonication process to maintain the temperature
178 of the fluid. This break avoids the nanofluid to heat up and losing the properties of particles, this
179 process followed for single nanoparticle dispersion as well. For hybrid nanoparticles, the weight
180 of nanoparticles was validated using Eq (2).

$$181 \quad W_{G-CNC} = \left(\frac{\varphi}{100-\varphi} \right) \times \left(\frac{\rho_{(GNP/CNC)}}{\rho_{(bf)}} \right) W_{bf} \quad (2)$$

182 Where 'W' is weight of hybrid nanoparticles 'φ' implies the concentration of single/hybrid
183 nanofluids by volume, 'w' stands for weight and 'ρ' defines the density. The subscripts 'GNP'
184 denotes Graphene nanoplatelets, 'CNC' is cellulose nanocrystal, 'bf' represents base fluid,
185 respectively. Figure 2 below provides a schematic illustration of the development of nanofluid.



186

187 Figure 2 Two-step method preparation method representation [26].

188 **2.3 Measurement devices**

189 **2.3.1 Evaluation of stability**

190 The clustered nanoparticles get agglomerated and interrupt the hybrid nanofluids stability due to
 191 their large surface area, which is a critical condition for their utilization. The GNP/CNC
 192 nanoparticles stability and dispersibility in the nanofluids were evaluated applying the method of
 193 sedimentation with photographs captured at different periods, and by using UV–Vis spectroscopy,
 194 and Zeta potential analysis. The spectrum was obtained using PerkinElmer's LAMBDATM
 195 UV/Vis with operational array of UV-spectrometer wavelengths of 200 nm–800 nm and specific
 196 cuvettes (quartz) appropriate for measuring light absorption for all the samples. For proper light
 197 transmission, all the samples with base fluid are diluted. The single / hybrid nanofluids Zeta
 198 potential is determined using the Anton Paar light sizer 500. In nanofluid dispersion, the

199 measurement of zeta potential displays the repulsion degree between nearby particles with the
200 same charge.

201

202 **2.3.2 Characterization**

203 The characterization of nanoparticles microstructure in the nanofluids is done using a transmission
204 electron microscope (TEM). The size of the particle and dispersion of W/EG developed GNPs and
205 hybrid nanofluids of GNPs were measured using a digital TEM. Before TEM examination, the
206 samples of the hybrid nanofluids are sonicated for 15 minutes. The TEM apparatus (Tecnai G2 20
207 S-TWIN, USA) with 210KV of accelerating voltage evaluated the solution of nanofluid constituted
208 of GNPs and CNC of the nano-base fluid. GNPs and CNC nanofluids were analyzed using an X-
209 ray diffractometer (Rigaku D/MAX-2500PC, Japan) with Cu K α radiation ($\lambda= 1.54056 \text{ \AA}$) at 40
210 KV and 30 mA, with 0.02/s rate of scan. The nanoparticle's phase was assessed using X-ray
211 Diffraction (XRD) analysis. The produced nanofluid trials are coated to assess the superficial
212 morphology for microstructure characterization. SEM scanning electron microscopy
213 (HITACHI/TM 3030 PLUS, Czech Republic) was used to examine the dispersion of nanoparticles
214 in the fluid. Field emission scanning electron microscopy (FESEM, Zeiss Sigma HD VP,
215 Germany) was used to examine the structure of developed filaments at 0.5 kV acceleration voltage.
216 Prior to observation, each sample has platinum sputtered. The samples were morphologically
217 inspected before being seen using a FESEM scope for capturing the topographical representations
218 of the powder as received [27, 28].

219 **2.3.2.1 Thermal conductivity measurement**

220 Various strategies for evaluating the thermal conductivity of nanofluids have been proposed in
 221 recent years. Transients hot-wire is the highly accurate and quick of all these approaches (THW).
 222 In this research, for the measurement of thermal conductivity a hot wire-type KD2-Pro (Decagon
 223 devices Inc., USA) is used for GNPs/ base fluid(W/EG), GNP-CNC/ based hybrid nanofluid is
 224 established. The below Table 1 gives the list of studies that indicates the thermal conductivity
 225 estimates obtained by authors at distinct volume concentrations. These values of thermal
 226 conductivity are used to validate with the thermal conductivity estimates attained in the present
 227 study at different temperatures and volume concentrations.

228 **Table 1:** Nanofluids Thermal Conductivity Enhancement Summary.

NP's	Conc- Wt (%)	Surfactant	Thermal Conductivity(W/m-K)				References
			30 °C	40 °C	50 °C	60 °C	
Graphene nanoplatelets	0.1	SDS	0.559	0.618	N/A		[29]
		CTAB	0.635	0.648			
		SDBS	0.64	0.66			
		Gum Arabic	0.645	0.676			
Graphene nanoplatelets	0.01	-	0.31	0.34	0.36	0.37	[30]
	0.05		0.38	0.4	0.41	0.42	
	0.1		0.43	0.44	0.45	0.46	
	0.2		0.46	0.48	0.5	0.52	
Graphene	0.05	-	1.02	1.019	1.03	N/A	[31]
	0.08		1.052	1.066	1.078		

Graphene oxide	0.1	SDS	0.63	0.65	N/A		[32]
		TX-100	0.62	0.64			
Graphene	0.124	Not used	0.315	0.318	0.319	0.325	[33]
	0.207		0.324	0.327	0.33	0.339	
	0.395		0.335	0.339	0.342	0.345	
Graphene nanoplatelets	0.02	Gum acacia	0.63	0.66	N/A		[34]
	0.1		0.72	0.77			
Carboxyl graphene	0.04	SDS	-	0.383	0.385	-	[35]
Graphene nanoparticles (750m ² /g)	0.024	Not used	0.68	0.71	N/A		[36]
	0.05		0.71	0.75			
	0.1		0.75	0.8			
Graphene NP-Ag	0.2	Not used/Acid treatment	0.63	0.651	N/A		[37]
	1.0		0.72	0.77			
Graphene nano-platelets	0.1	NPE 400 (ionic)	0.5	0.51	0.525	N/A	[38]
	0.2		0.54	0.55	0.565		
	0.3		0.62	0.64	0.66		
Graphene nanoplatelets	0.01	Gum Arabic	0.63	0.64	0.657	0.663	[39]
	0.05		0.64	0.642	0.67	0.682	
	0.1		0.641	0.68	0.7	0.712	
Graphene nanoplatelets	0.1	Not used	0.187	0.18	0.179	0.17	[40]
	0.25		0.20	0.20	0.199	0.19	

	0.5		0.215	0.213	0.21	0.209	
Graphene nanoparticles	0.25	SDBS	0.40	0.405	0.419	0.42	[41]
	0.5		0.41	0.415	0.421	0.43	
	1.0		0.42	0.425	0.435	0.44	

229

230 **Table 2:** Physical form of Properties of Nanoparticles. (Nanografi nanotechnology (USA), MY
 231 Biomass Sdn. Bhd (MALAYSIA))

Properties	GNP	CNC
Color	Black	White (dry powder)
Purity	99.9%	-
Density (kg/m ³)	2267	1050
Structure	Platelet shaped sheets	Crystalline form
Specific surface area (m ² /g)	800	-

232

233 **Table 3:** Thermophysical Properties at 20 °C temperature of base fluid [42, 43].

Properties	Water	Ethylene glycol
Chemical formula	H ₂ O	C ₂ H ₆ O ₂
Vapor pressure (kPa)	3.169	0.007
Molar mass (g/mol)	18.0153	62.07
Density (kg/m ³)	1000	1100

234

235 A temperature bath (WNB7-MEMMERT, Germany) is used to sustain and monitor the thermal
 236 conductivity measurement by the temperature control. Probe vibration must be regulated to
 237 minimize experimental errors. To position vertically the KS-1 probe in the middle point of the
 238 sample vial, a horizontal support was mounted adjacent to the temperature bath. To examine the
 239 reproducibility of the data, the measurements were repeated twenty times in all planned volume
 240 concentrations and temperatures with a 5-minute intervening period. The Table 2 shows the
 241 physical properties of selected Graphene nanoplatelets and CNC nanoparticles, and Table 3 gives
 242 the information about the thermophysical Properties of base fluid water and ethylene glycol at 20
 243 °C temperature. Table 4 presented few specifications of thermal conductivity measuring device
 244 KD2 Pro information.

245

246 **Table 4:** Specifications of thermal conductivity measurement device (KD2 Pro).

Accuracy $\pm 5\%$	Thermal conductivity
Range of operation	0–50 °C
Range of measurement	0.02–2 W/m K
KS-1 Sensor	Needle length: 60 mm
	Needle diameter: 1.3 mm

247

248 **2.3 Viscosity**

249 Rheometer was used to assess the viscosity of all nanofluids in the range of 20 to 50 °C temperature
 250 at a constant shear rate (Brookfield DV-I prime viscometer) with varying volume concentrations.

251 A circulating water jacket is connected to an RST coaxial cylinder rheometer to assess the

252 temperature range and other uses. The rheometer can measure viscosities from 0.0001 to 5.4x106
253 Pa. s and temperatures from -200 to +180 °C. Experiment was carried out in a steady-state
254 environment. Rotational measurement with a controlled shear rate was used as the method of
255 measurement. To authenticate the rheometer, the base fluids viscosity was quantified, and the
256 results were assessed to ASHRAE standard data. The viscosity is measured with 15.7 mL of fluid,
257 and the results are compiled in a computer connected to an RST rheometer. To reduce the
258 experimental error, five precision readings were acquired and averaged. Previously, several
259 researchers used the Brookfield rheometer to determine viscosity [44-46]

260

261 **2.4 Density & Specific heat measurement**

262 The pumping power, friction factor, Reynolds number, and other properties of nanofluids are all
263 affected by density. In this work, a digital density meter was employed to test the density of GNPs
264 & GNP/CNC nanofluids with varying volume concentrations, similar to prior investigations by
265 various researchers. The density meter used here is a KEM (model DA-640) from Kem Kyoto
266 Electronics Co. Ltd. The density (gm/cm³) measuring range on this meter is 0.0000-3.000, with a
267 ±0.0001gm/cm³ precision along with repeatability of 0.00005 density (gm/cm³). The temperature
268 range for utilizing this meter is upto 35 degrees Celsius, with a humidity level of 85 percent RH
269 or less. The density is measured using an ASTM D4052-18 digital density meter, which is
270 recognized as a standard test method for density, relative density, and API gravity of liquids[47-
271 49]. Differential Scanning Calorimetry (DSC) is a sensitive method for determining the specific
272 heat capacity of viscoelastic fluids. PerkinElmer, Inc.'s DSC (model DSC 8000) was utilized to
273 measure the specific heat in this study. The specific heat capacity of base fluid and GNP's/CNC
274 nano fluids was examined at room temperatures. The measurement solution was placed in an

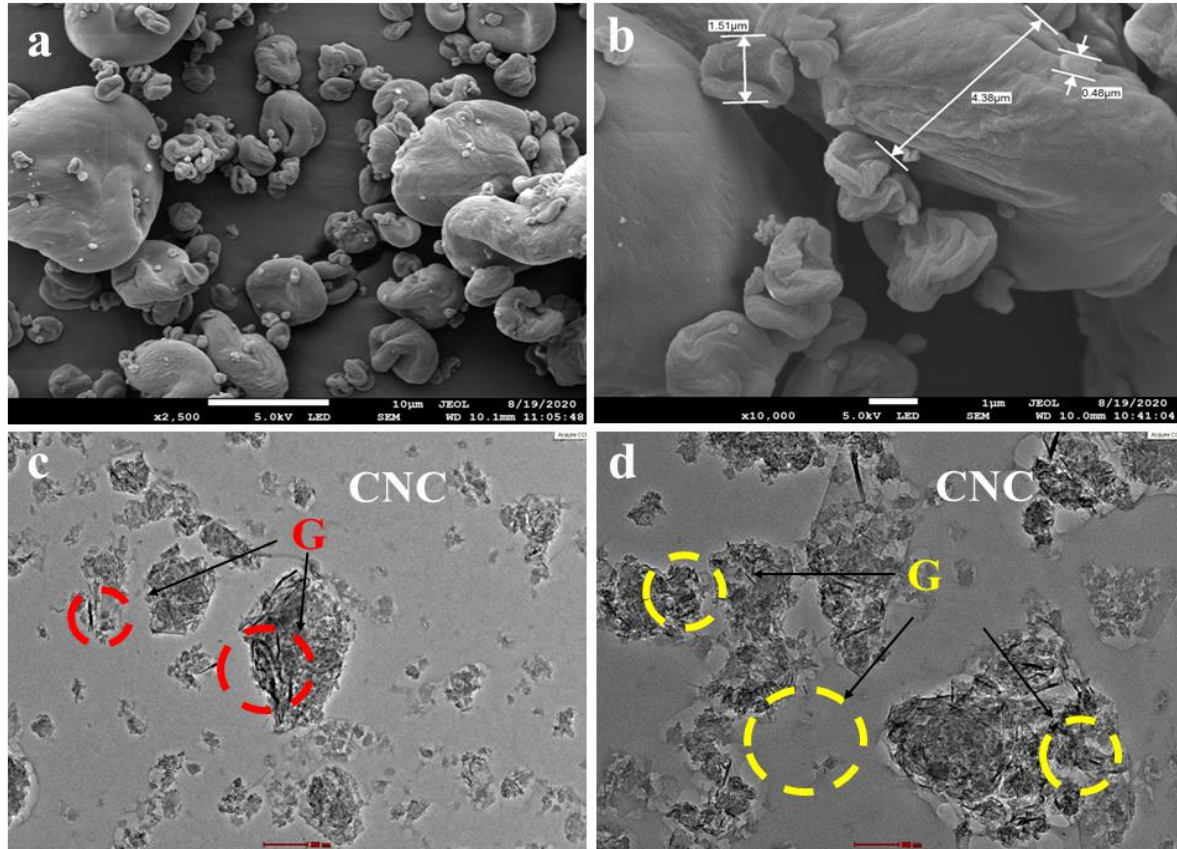
275 aluminum pan and weighed on an electrical balance with precision: 0.0001 before being covered
276 with an aluminum lid and sealed with a universal crimper press. An empty pan filled with sapphire
277 reference were placed in DSC before the actual sample measurement to get baseline and reference
278 data. Following that, the sample pan was put in DSC beside an empty pan as a control. Following
279 the standard DSC test procedure ASTM-E1269. the temperature range was set with a 100C/min
280 temperature difference. For each sample, a minimum of 6 minutes was required. This test was
281 carried out for all nanofluid and base fluid volume concentrations. The generated values are saved
282 on a computer that is linked to DSC. Many previous studies employed DSC to conduct precise
283 heat measurement tests on nanofluids[50-53].

284 **3 Results and Discussions**

285 **Nanofluid preparation, characterization, and stability**

286 The preparation method used is two step method for single graphene nanoplatelets, and hybrid
287 nanoparticles dispersal. In the Faculty of Mechanical Engineering's Advanced Automotive Liquid
288 Lab (A2LL) at University Malaysia Pahang, the needed graphene nanoplatelets & nanocellulose
289 hybrid nanofluid was prepared successfully. Over a 5-hour ultrasonication duration followed by
290 magnetic stirring, ultrasonication is the most influential way for generating very balanced
291 dispersion of GNPs and hybrid nanoparticles. Figure 4 displays diffraction peaks for the CNC and
292 graphene refraction planes, respectively, at $2\theta = 15.7^\circ$, 22.8° , 34.6° and 26.3° , 43.9° , 54.1° . The
293 peak in graphene at $2\theta=26.35^\circ$ reflected a typical graphitic carbon diffraction pattern [37, 54, 55].
294 Furthermore, the connected carbon in cellulosic form was demonstrated by a negatively diffracted
295 signal at 22.8375° . Further shows that the CNC peak intensity is higher to that of the peak of the
296 graphene. The FESEM images for GNP and CNC are shown in Figure 3(a & b). A consistent
297 dendrite forms uneven structure noticed for GNPs with platelet structure and CNC with porous

298 microstructure with homogeneity and uniformity. TEM examination of CNC and GNP
299 nanoparticle morphology and dispersion depicts in Figure 3 (c & d). It shows clearly distributed
300 GNPs together with a CNC base due to the transparency. The images show that as the
301 concentration of nanoparticles increased, resulting in a reduction in clarity, suggesting
302 agglomeration. The structure of cellulose nanocrystals and the dispersion of graphene
303 nanoplatelets in the base fluid (EG/W) is investigated using microstructure TEM
304 analysis. Graphene platelet structure and CNC with a clear and gentle exterior in the base fluid,
305 displaying the fragile structure behaviour. Finally, the morphology of the dispersed GNPs and
306 CNC reveals that the nanoparticles were well prepared and dispersed in the ethylene glycol and
307 water base fluid. The information more related to the preparation of the nanofluid in detail can be
308 found in the previous article by authors related to preparation, characterization and permanence
309 (stability) of the single and hybrid nano fluid that is prepared [56].

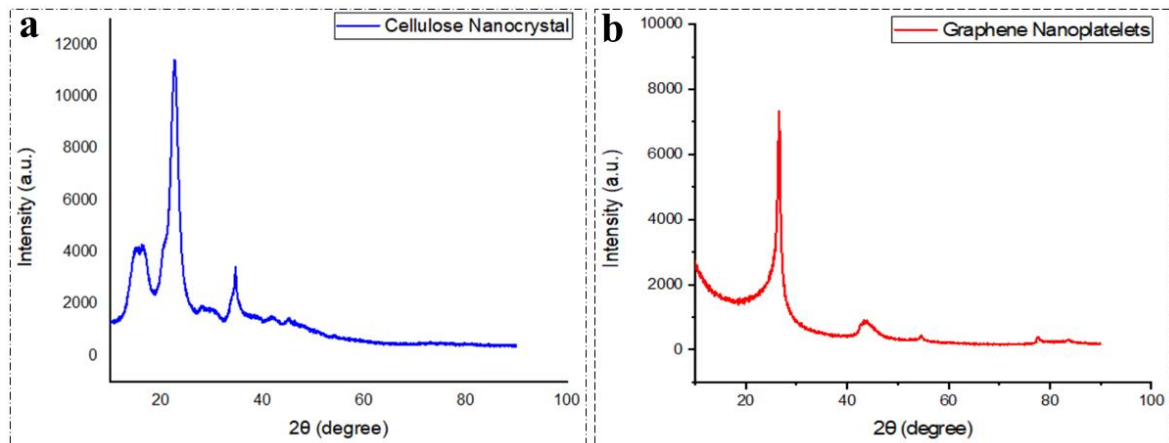


310

311 Figure 3 Images of FESEM of (a) GNP's-Graphene nanoplatelets with CNC hybrid nanofluid

312 at 2500x (b) at 10000x magnification. (c) TEM images of hybrid nanofluids 0.2% GNP/CNC

313 at lower enlargement, (d) at higher magnifications.



314

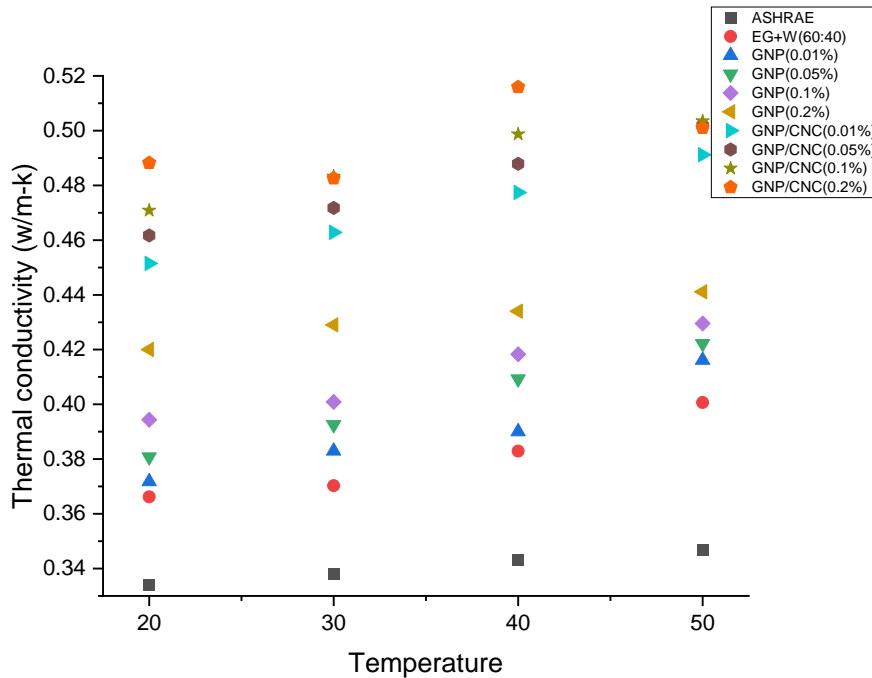
315 Figure 4 Analysis of XRD (a) CNC and (b) Nanoparticles of Graphene nanoplatelets.

316 3.3 Thermal conductivity

317 Thermal conductivity was measured by using the KD2 Pro thermal properties analyzer in the
318 temperature range of 20–50 °C. Validation is a process of calculating the parameters in any
319 laboratory work, for this the instrument must be adjusted. To calibrate the unit, the KD2 Pro
320 Manufacturer recommends using a standard sample of glycerin. The accuracy of the measurement
321 device must be tested as a condition before calculating the final thermal conductivity tests of nano-
322 fluid. Besides the measured data for base fluid was compared with the data presented by different
323 authors [29, 57]. As expected, the previous research suggests that the thermal conductivity value
324 increases as the temperature increases, with a maximum inaccuracy below 10 percent, the KD2
325 Pro over/ underestimated the recorded values of thermal conductivity. The effect of temperature
326 and the concentration based on volume for the thermal conductivity of graphene and hybrid
327 GNPs/CNC nanofluids has been extensively investigated. The different volume percentages have
328 variable thermal conductivity. GNP/CNC hybrid nanofluid samples are tested at temperatures
329 ranging from 20 to 50 degrees Celsius as shown in Figure 5. The thermal conductivity of graphene
330 nanofluids is shown in Fig. as a function of concentration in the range of 0.01–0.2 vol. percent at
331 various temperatures. To avoid an increase in effective viscosity and sedimentation, low weight
332 percentages are chosen. The thermal conductivity increases as the concentration of Graphene
333 increases, which is to be expected. At a concentration of 0.01 % the thermal conductivity value is
334 0.3716 W/m-K for graphene nanoplatelets nanofluid at 20°C. At a concentration of 0.2 percent, the
335 maximum enhancement was 27 percent with 0.4411 W/m-K at 50 °c. At the same temperature,
336 from image contrasts the enhancement of thermal conductivity with concentrations of graphene
337 and hybrid Graphene nanofluids. It is clear that the rate of enhancement increases with
338 concentration of graphene and Cellulose nano crystals in comparable to metallic and ceramic

339 nanofluids and is much superior to them. Temperature and volume concentration significantly
340 increase the thermal conductivity of graphene nanofluids.

341 This is due to the fact that graphene nanofluids contain particles of varying sizes. In accordance
342 with percolation theory, the larger particles contribute to the formation of a network-like chain
343 structure. Brownian motion is contributed by the smaller particles, which travel spontaneously. As
344 the temperature rises, Brownian motion creates micro convection, which provides thermal
345 conductivity to increase. This has led to the strong suggestion of a hybrid character for thermal
346 conduction in graphene nanofluids comprising micro convection and diffusion phenomena. With
347 increases in both the weight proportion and the temperature, the rise in thermal conductivity is
348 nonlinear. The nonlinearity/linearity of the variability of thermal conductivity with respect to
349 weight fractions is influenced by the characteristics of the hybrid nanoparticle and even the base
350 fluid. The increase in thermal conductivity is 14.91 percent at 20 °C and about 17.77 percent at 40
351 °C when using a 0.01 percent weight concentration of GNP–CNC nanofluid. The high thermal
352 conductivity of GNP and CNC nanoparticles results in an increase in effective thermal
353 conductivity. The spacing amongst nanoparticles (unrestricted passage) reduces as the volume
354 fraction of nanoparticles increases. It occurs as a result of the percolation effect.



355

356 **Figure 5:** Thermal conductivity of GNP & GNP/CNC nanofluids at different concentrations and
 357 temperature

358 Other studies have also seen an increase in thermal conductivity of carbon-based nanofluids as the
 359 weight concentration increases.[58, 59]. To explain the reason for thermal conductivity of
 360 nanofluids has increased so dramatically, Nanoparticles move in a Brownian approach, and the
 361 liquid at the liquid/particle contact layers at the molecular level, the nature of heat transmission to
 362 the nanoparticles, and the impact of nanoparticle clustering are some of the hypothesized
 363 mechanisms [60]. They reached the conclusion that Brownian motion can be ignored because
 364 thermal diffusion has a greater influence than Brownian diffusion though it is the measure
 365 of immobile nanofluids. Although many contributing factors have been examined, such as the
 366 liquid–solid interfacial region, Brownian motion, charge carrier status, and ballistic dielectric
 367 transport, no overarching mechanism to govern the exceptional behaviour patterns of nanofluids,
 368 including that of the significantly improved effective thermal conductivity, has been discovered.

369 Similar to the graphene nanofluid thermal conductivity there is an increase in the hybrid GNP/CNC
 370 hybrid nanofluids with increase in volume concentration from 0.01 % to 0.2%. At 40 °C for 0.2%
 371 the thermal conductivity value is recorded as 0.465 W/m-K. At same volumetric concentration and
 372 temperature in comparison with single and hybrid nanofluid there is an increase of 5.2 % and 13.3
 373 % with respect to base fluid. Below table 5 gives the validation of present study by comparing it
 374 with the previous studies based on graphene nanoparticles and hybrid nanoparticles. The present
 375 study base fluid experimental values at 60:40 EG:W ratio, agrees well with the author Sundar,
 376 Singh [61] at same base fluid ratio at the temperatures varying from 20 to 50°C. The thermal
 377 conductivity values are compared at around equal concentrations and temperature to give a clearer
 378 vision of the present study.

379 Table 5: Thermal conductivity of single and hybrid nanofluids attained by various researchers.

Nanoparticle	Concentration/ Temperature	k_{NF}/k_{BF}	References
Graphene nanoplatelets/EG- W	$\phi = 0.01\% \text{ vol./}50 \text{ }^\circ\text{C.}$	1.038	Present study
	$\phi = 0.05\% \text{ vol./}50 \text{ }^\circ\text{C.}$	1.053	Present study
	$\phi = 0.1\% \text{ vol./}50 \text{ }^\circ\text{C.}$	1.071	Present study
	$\phi = 0.2\% \text{ vol./}50 \text{ }^\circ\text{C.}$	1.100	Present study
Graphene nanoplatelets- CNC/EG-W	$\phi = 0.01\% \text{ vol./}50 \text{ }^\circ\text{C.}$	1.225	Present study
	$\phi = 0.05\% \text{ vol./}50 \text{ }^\circ\text{C.}$	1.252	Present study
	$\phi = 0.1\% \text{ vol./}50 \text{ }^\circ\text{C.}$	1.256	Present study
	$\phi = 0.2\% \text{ vol./}50 \text{ }^\circ\text{C.}$	1.250	Present study
3D-Graphene/EG	$\phi = 0.1\% \text{ wt./}25 \text{ }^\circ\text{C.}$	1.149	Bing, Yang [62]
Graphene/DIW	$\phi = 0.1\% \text{ wt. /}25 \text{ }^\circ\text{C}$	1.416	Ghozatloo, Rashidi [63]

Nanoparticle	Concentration/ Temperature	k_{NF}/k_{BF}	References
Graphene nanoplatelets/EG	$\phi = 0.5\%$ vol./ 35 oC	1.208	Selvam, Lal [64]
		1.160	
	$\phi = 0.1\%$ wt./60 °C (500 m2/g GNPs)	1.287	Iranmanesh, Mehrali [65]
$\phi = 0.1\%$ wt./60 °C (750 m2/g GNPs).	1.307		
Graphene/EG/DIW	$\phi = 0.2\%$ wt./25 °C.	1.092	Contreras, Oliveira [66]
Graphene nanoplatelets	$\phi = 1\%$ wt./25 °C (750 m2/g)	1.211	Wang, Wu [67]
Hybrid-Graphene wrapped MWNT			
TiO ₂ /Graphene/W	$\phi = 0.25\%$ vol./25 °C.	1.098	Bakhtiari, Kamkari [68]
	$\phi = 0.25\%$ vol./55 °C.	1.138	
Al ₂ O ₃ /Graphene oxide/W	$\phi = 0.25\%$ vol./50 °C.	1.125	Taherialekouhi, Rasouli [69]
Fe-Si/DW	$\phi = 0.25\text{wt } \%/50$ °C.	1.109	Huminić, Huminić [70]
Graphene oxide/Co ₃ O ₄ /W	$\phi = 0.2\text{wt } \%/50$ °C.	1.156	Sundar, Singh [61]
Graphene oxide/Co ₃ O ₄ /EG	$\phi = 0.2\text{vol } \%/50$ °C.	1.113	Sundar, Singh [61]
Graphene oxide/Co ₃ O ₄ /EG/W	$\phi = 0.2\text{vol } \%/50$ °C.	1.120	Sundar, Singh [61]
Graphene oxide-CuO/EG-W	$\phi = 0.2\text{vol } \%/50$ °C	1.094	Rostami, Nadooshan [71]
Graphene nanoplatelets-platinum/DW	$\phi = 0.1\text{vol } \%/40$ °C	1.174	Yarmand, Gharekhani [27]

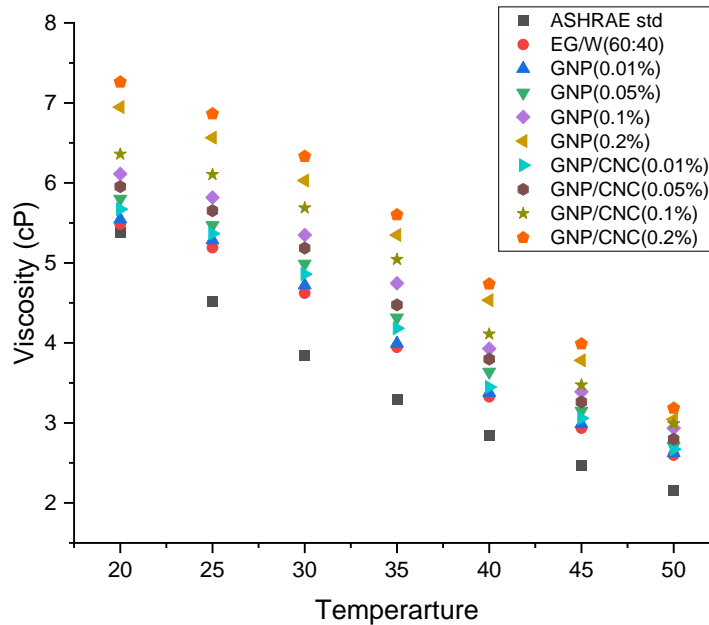
380

381 3.4 Viscosity

382 The viscosity of EG/ distilled water (base fluid) at a ratio of 60:40 and GNP/CNC hybrid
383 nanofluids at varying volume concentrations and temperatures ranging from 20 to 50 °C is shown

384 in Figure 6. The viscosity has adverse effects on two factors for pressure drop and pumping power
385 constraints, similar to density. Because of NPs/surface collisions and other inter-layer resistance
386 and interfacial forces, the presence of Nano Particles in the Base fluid, i.e., constituting to the
387 Nanofluid it increases friction at the fluid/surface contact. At 20 °C, the measured viscosity of the
388 base fluid (EG/Water) is 5.485 (mPa-s), which is consistent with literature values. Since the
389 increasing concentration has a direct effect on the fluid internal shear rate, the viscosity of
390 nanofluids rises as the volume fraction of nanofluids rise [72]. The viscosity reduces as the
391 temperature rises, as the intermolecular and interparticle adhesion forces weaken. When 0.2
392 percent volume concentration of GNP nanofluid is compared to the viscosity of EG/Water at 20
393 °C, the viscosity increases by around 21%. Similarly, there is an increase in viscosity by 24.5 %
394 at 0.2 volume concentration of hybrid nanofluid (GNP/CNC) at 20°C. The viscosity values
395 diminish as the temperature rises. The increased viscosity value at 0.2 percent volume
396 concentration of GNP nanofluid at 50°C is only 14.7% as compared with base fluid and hybrid
397 nanofluid of GNP/CNC at 0.2% volume concentration at 50°C is 18.3%. The GNP/CNC sample
398 had the highest stability and caused the greatest increase in average viscosity of the base fluid.
399 High colloidal stability and the lowest rise in base fluid viscosity are two of the most important
400 factors to consider when using nanofluids as operating fluids in the applications of heat transfer.
401 Accordingly, by the viscosity values the highest concentration of nanoparticles (single/hybrid) can
402 be considered to be effective.

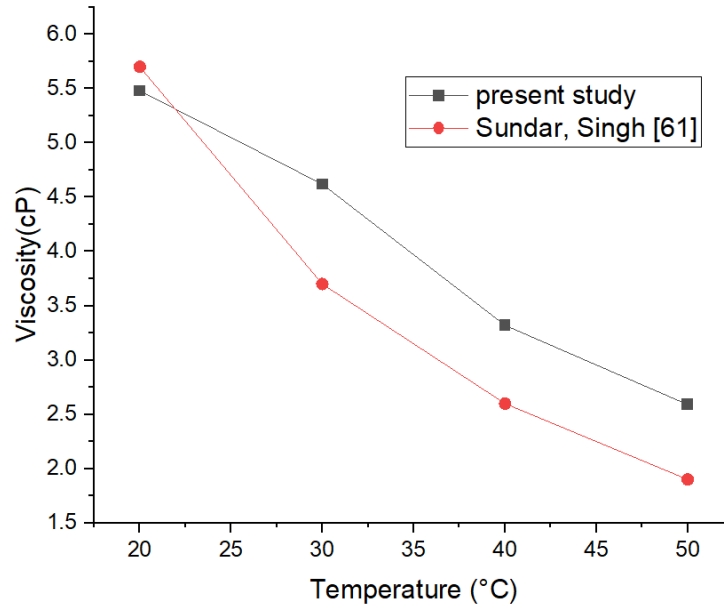
403



404

405 **Figure 6:** Viscosity of prepared nanofluids at different concentrations and temperature

406 Because a huge amount of nanomaterial has been disseminated, the friction factor appears to be
 407 high at high volume concentrations. The friction factor, literally, improves the value of dynamic
 408 viscosity. However, as the temperature of the nanofluid rises, the intermolecular adhesion force
 409 weakens, resulting in a lower dynamic viscosity value [73]. Figure 7 depicts the viscosity ratio of
 410 60:40 (EG:W)-based fluids, as well as from author Sundar, Singh [61] data for 60:40 (EG: W)
 411 based fluids for the comparison of the study. The viscosity of the 60:40 (EG: W) fluid is found to
 412 be nearly identical throughout a wide range of temperatures.



413

414 Figure 7: Viscosity comparison of prepared base fluid at different temperatures

415

416 3.5 Density

417 The volume concentration of nano particles and the distilled water with ethylene glycol base fluid
 418 equals the density of nanofluids. The base fluid has an impact on the nanofluids density. The
 419 density of nanofluids is also affected by temperature. The density of nanofluids drops as the
 420 temperature rises. Figure 8 shows the density of nanofluids determined at 20°C for the base fluid
 421 and varying volumetric concentrations of GNPs & GNP/CNC nanofluids. The result of density of
 422 base fluid is in good quality agreement with ASHRAE data and the deviation is below 1%. Table
 423 2 shows theoretical density values for a range of fluids. The difference between experimental and
 424 theoretical density data is less than 1.0 percent, indicating that the two types of density values of
 425 base fluid and nanofluids are in good agreement. The density measurements of the nanofluids are
 426 compared to the projected values using Eq. (3), with the density of GNP, CNC, and base fluid

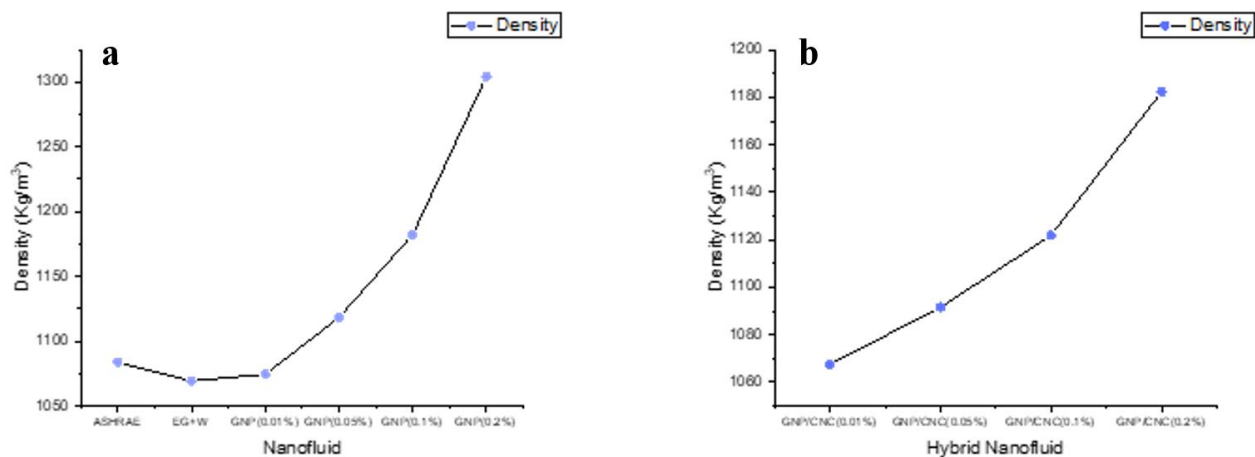
427 being 1065 kg/m³ ,1072 kg/m³ and 1060 kg/m³, respectively. The density of the nanofluid changed
428 in direct proportion to the nanoparticle concentration in comparison to the base fluid.

$$429 \quad \rho_{nf} = \phi\rho_s + (1 - \phi)\rho_f \quad (3)$$

430 Where ‘ ρ ’ denotes the density, is ‘ ϕ ’ volume concentration, the subscripts ‘nf’ is nanofluid, ‘s’ is
431 solid nanoparticles, ‘f’ is the base fluid (W/EG)

432 According to the molecular dynamic simulation principle, the nanoparticles are filled with the
433 molecules of the base fluid in various ways. In the case of nanofluids, increased Vander wall
434 interaction causes non-uniform density to change in the interfacial region being the disparity in
435 reported data. The density value is decreased for hybrid nanofluids (GNP/CNC) when compared
436 with single nanofluid (GNP). The density value of Graphene nanoplatelets at 0.2 % volume
437 fraction is 1304.2 Kg/m³ & at same volume fraction for hybrid nanofluid of graphene
438 nanoplatelets/cellulose nanocrystals (GNP/CNC) is 1182.32 Kg/m³ respectively. It clearly shows
439 density value increases with volume concentration. The density of base fluid (water/ethylene
440 glycol) in comparison with 0.2% concentration of Graphene nanoplatelets is 18.6% and at same
441 concentration and temperature of hybrid nanofluid it is 10.23%. This confirms that density
442 decreased for hybrid nanofluid when compared with single nanofluid composition. Table 6
443 representing theoretical density values of fluids. The density of hybrid nanofluid increases as the
444 volume concentration of nanoparticles increases and the temperature decreases. The nanofluid
445 with a 0.02 % volume concentration and 70:30 Cu-GNPs hybrid nanoparticles had the maximum
446 density in a research conducted by Kishore, Sireesha [74]. similar equation as in this study is used
447 to compute the density of hybrid nanoparticles by the author. Because copper has a higher density
448 than graphene, the densities of 70:30 Cu-GNPs is higher with respect to the author. A hybrid
449 nanofluid's density is influenced by both the volume percentage and the densities of the

450 nanoparticles. Following the similar trend in this research study, the density of the Graphene
 451 nanoplatelets in single nanoparticle fluid is higher compared to hybrid nanofluid as shown in the
 452 below figures of experimental density.



453
 454 **Figure 8:** Density of nanofluids at different concentrations a) Graphene nanoplatelets b) Hybrid
 455 GNP/CNC

456 **Table 6:** Theoretical density values of fluids

Fluids		Density (kg/m ³)	
EG+ Water (60:40)			
0.01% GNP	0.01% GNP/CNC	1052.2	1105.5
0.05% GNP	0.05% GNP/CNC	1101.3	1127.9
0.1% GNP	0.1% GNP/CNC	1162.7	1155.2
0.2% GNP	0.2% GNP/CNC	1285.4	1211.7

457

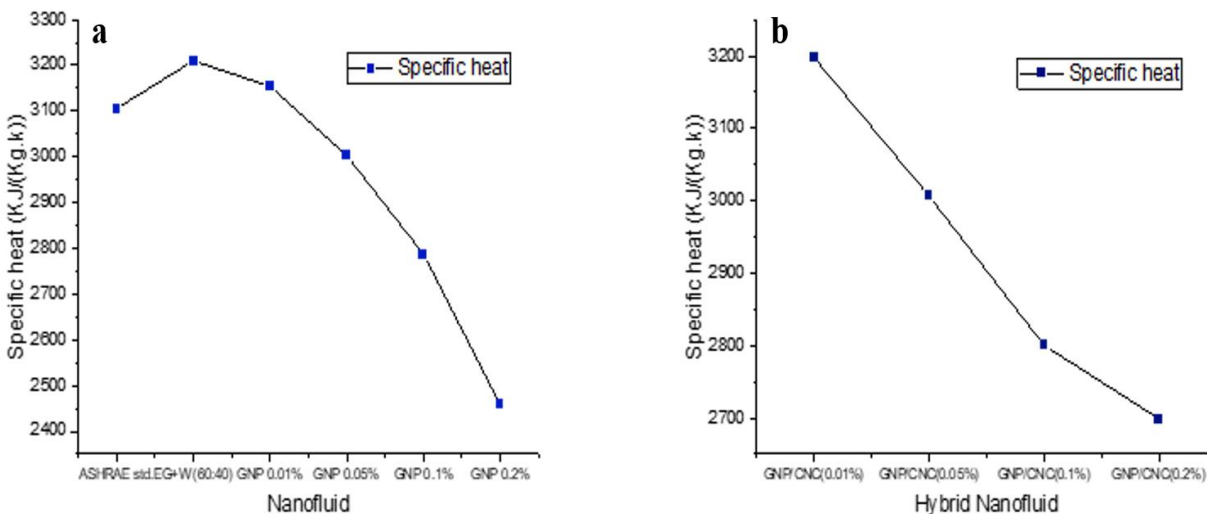
458 **3.4 Specific heat**

459 Differential Scanning Calorimetry was used to investigate the specific heat capacity characteristics
460 of CNC nanofluids. Figure 9 shows the specific capacity of the base fluid and GNP & GNP/CNC
461 nanofluids. Figure (b) depicts the effect of temperature and mass fraction on specific heat capacity
462 when the GNP/CNC mass ratio is 1:1. There have not been enough mathematical and
463 investigational research to estimate the nanofluids specific heat capacity at various temperatures
464 and volume concentrations. The specific heat capacity of nanofluid samples is lower than that of
465 base fluid, as can be observed from Figure 9. The specific heat capacity of particles decrease as
466 their volume concentration increases. At 30 °C, the measured specific heat capacities of nanofluids
467 demonstrate that they are roughly 0.56 percent and 7.52 percent lesser than those of the base fluid
468 for 0.01 and 0.2 volume percent of nanoparticles, respectively. However, most previous studies
469 have shown that adding nanoparticles reduces the specific heat capacity, although some
470 unexpected outcomes have also been recorded [75]. The heat capacity of nanofluids appears to be
471 affected by the specific heat capacity of both nanoparticles and the base fluid, and the interfacial
472 energy released of solid liquid is altered when suspended nanoparticles are adjusted. The specific
473 heat of nanocomposite materials is influenced by the surface free energy of nanoparticles since
474 they have a higher surface area and a greater overall heat capacity. On one hand, this is due to the
475 fact that water has a higher specific heat than nanoparticles; on the other hand, it demonstrates that
476 the hybrid nanoparticle has a significant impact on specific heat capacity; even a small amount of
477 mass fraction nanoparticle can significantly reduce specific heat capacity, especially at lower
478 temperatures. The specific heats of the hybrid and single nanoparticle nanofluids, GNP-EG/W
479 nanofluid and GNP/CNC-EG/W nanofluid, with the same mass fraction nanoparticles of 0.1
480 percent, are contrasted in both images. It means that as the temperature rises, all specific heat
481 capacities rise as well. Besides water, it is seen that hybrid nanofluid has the highest specific heat.

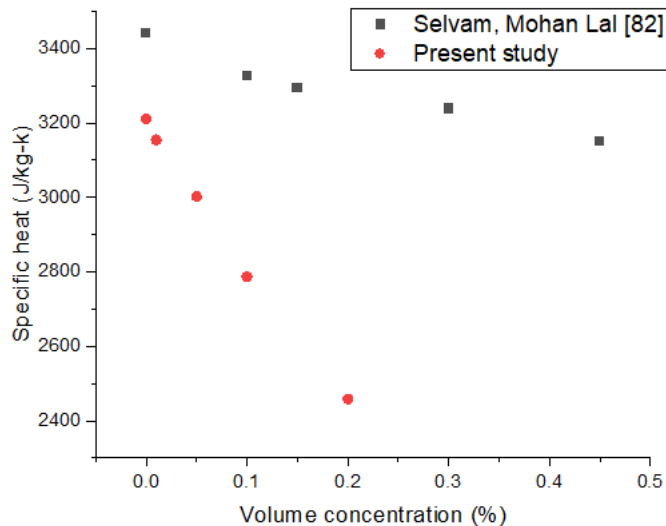
482 This is owing to the GNP's low specific heat capacity and the nanofluid's lower GNP/CNC
483 concentration.

484 The specific heat capacity of the 0.01 and 0.2 volume % for mono nanofluid (GNP) reduces by
485 1.74% and 23.43 % as compared to the base liquid, respectively. The specific heat of the hybrid
486 nanofluid (GNP/CNC) reduces by 0.38 % as compared at 0.01 wt.% and it reduces by about 15.92%
487 at 0.2 wt%. The specific heat value when compared between Hybrid Nanofluid (GNP/CNC) and
488 mono nanofluid GNP at 0.01 wt% is increased by 1.35% and at 0.2 wt% is increased by about
489 8.92%. It can be concluded that specific heat value is much higher for hybrid nanofluid than mono
490 nanofluid at lower volume concentration. The Specific Heat Capacity of hybrid nanofluids has
491 been demonstrated to be significantly affected by temperature. The reduced Specific Heat
492 Capacity of hybrid nanofluids compared to water is universally agreed upon by all studies [76].
493 According to a study temperature has a mixed effect on specific heat that is rather inconsistent.
494 Fazeli, Emami [77] found that as the temperature of the MWCNT-CuO increased from 20 to 35
495 °C, the Specific heat capacity of the MWCNT-CuO reduced. A similar finding was made by
496 Mousavi, Esmailzadeh [78] who found that the CuO/MgO/TiO₂ triple hybrid nanofluid had a
497 decreasing SHC as temperature increased across all volume concentrations studied. Few authors
498 explained the effect of volume concentration on specific heat capacity of hybrid nanofluids that it
499 exhibits a linear relationship with the volume concentration of hybrid nanofluids. The combined
500 influence of the specific heat capacities of the nanoparticles and base fluids is responsible for this
501 tendency. Furthermore, raising the volume concentration of nanoparticles appears to disrupt the
502 solid-liquid phase's interfacial free energy. Because nanoparticles have a bigger surface area, their
503 surface free energy has a stronger impact on overall heat power, which influences nanocomposite
504 materials' specific heat [18, 75, 76]. When volume concentration was improved from 0.02 percent

505 to 0.06 percent at the constant temperature of 20 °C, specific heat capacity decreased showing 7%
 506 drop [27]. Similar trend was recorded in different studies [79, 80]. Their research also found that
 507 when the volume concentration of the hybrid nanofluid increased, the specific heat capacity of the
 508 hybrid nanofluid decreased significantly. As liquids (base fluids) have a greater specific heat
 509 capacity than solids (nanoparticles), the base fluids have more hybrid nanocomposites added to
 510 them that affected the Specific heat capacity to drop, according to this analysis. When the volume
 511 concentration of the generated Graphene-Al₂O₃ hybrid nanofluid was increased 0.05 wt percent to
 512 0.15 wt percent (as relative to the base fluid -20 °C), Gao, Xi [81] reported a Specific heat capacity
 513 reduction of 4 to 7 percent. At 30°C, Figure 10 depicts the fluctuation of specific heat capacity in
 514 relation to the volume fraction of GNP loadings. The specific heat of nanofluid is shown to
 515 decrease as GNP loadings increase. Because GNP has a lower specific heat capacity than the base
 516 fluid, the specific heat capacity of the nanofluid decreased when GNP is added. The most
 517 significant reduction in specific heat is determined to be 8% by Selvam, Mohan Lal [82]. The
 518 decreasing trend of specific heat value similar to the present study is plotted in image to validate
 519 the present study.



521 **Figure 9:** Specific heat of nanofluids at different concentrations a) Graphene nanoplatelets b)
522 GNP/CNC



523

524 **Figure 10:** Comparison of graphene nanofluid Specific heat at different concentrations

525

526 4 Conclusion

527 A single & hybrid nanofluid of Graphene nanoplatelet (GNP) & GNP/CNC nanoparticles has been
528 prepared by using two step method. Later the characteristic properties and thermophysical
529 properties are studied at various volume concentrations in base fluid of EG/Water (60:40), with
530 volume concentrations of 0.01 %, 0.05%, 0.1%, and 0.2% and it was concluded that,

- 531 • All GNP–CNC hybrid nanofluid samples give an increase in thermal conductivity with
532 base fluid. At 0.2 vol % at 40 °C, experimental data reveals that thermal conductivity
533 enhanced by 27%. At the room temperature for GNP nanofluid the values of thermal
534 conductivity are in the range of 0.441W/m-K and for hybrid nanofluid in the range of 0.515

535 W/m-K. The viscosity of GNP/CNC nanofluids decreased with the increase in temperature.
536 At 0.2 % of GNP nanofluid, the viscosity increased by 21%. Similarly, there is an increase
537 in viscosity by 24.5% at 0.2% of hybrid nanofluid (GNP/CNC) at 20°C with comparison
538 to base fluid.

- 539 • The experimental density of nanofluid obtained was consistent with theoretical values. The
540 density value of GNP & GNP/CNC at 0.2 volume concentration is 1304.2 Kg/m³ &
541 1182.32 Kg/m³ respectively with an increase of 18.6% & 10.23% in comparison to base
542 fluid. With an increased nanoparticle volume fraction, the nanofluid's specific heat
543 capacity drops. At lower temperatures, the volume percentage of nanoparticles has a
544 greater impact on the specific heat of hybrid nanofluid. The specific heat decreased with
545 increase in nanoparticle concentration and when compared with Hybrid Nanofluid
546 (GNP/CNC) and single nanofluid there is an increase by 1.35% and 8.92% at 0.01 and 0.2
547 vol % respectively.

548 The thermophysical characteristics of GNPs & GNP/CNC nanofluids obtained as a result suggest
549 that this is an effective and useful approach for thermal engineering applications. Due to synergetic
550 effects, GNP/CNC hybrid-based nanoparticles revealed properties that could not be achieved by
551 using GNP or CNC nanoparticles independently. It is demonstrated that combining the diversity
552 and uniqueness of both GNP and CNC not only enhances the number of applications available,
553 but also provides undeniable benefits to their respective distinct characteristics. These hybrids have
554 a several features that make them suitable for sensing, electronics, optical, biomedical, energy
555 storage and heat transfer applications.

556 **CRedit author statement**

557 **M. Sandhya:** Conceptualization, Visualization, Investigation, Data curation, Writing- Original draft
558 preparation, Reviewing and Editing. **D. Ramasamy:** Supervision, Writing-Reviewing and Editing. **K.**
559 **Kadirgama:** Writing- Reviewing and Editing. **W.S.W. Harun:** Writing- Reviewing and Editing. **R.**
560 **Saidur:** Writing- Reviewing and Editing.

561

562 **Declarations**

563 **Competing interests**

564 The authors claim they are conscious and say no financial or personal conflicts that might have
565 affected the research provided in this study.

566

567 **Authors' contributions**

568 **M. Sandhya:** Conceptualization, Visualization, Investigation, Data curation, Writing- Original draft
569 preparation, Reviewing and Editing. **D. Ramasamy:** Supervision, Writing-Reviewing and Editing. **K.**
570 **Kadirgama:** Writing- Reviewing and Editing. **W.S.W. Harun:** Writing- Reviewing and Editing. **R.**
571 **Saidur:** Writing- Reviewing and Editing.

572

573 **Funding**

574 The authors gratefully acknowledge University Malaysia Pahang (UMP) for financial support and
575 facilities provided by Grant RDU 190194, FRGS/1/2018/TK03/UMP/02/26, and UMP Flagship
576 RDU192204. The authors would also like to be grateful for the resources supplied by the Sunway
577 university.

578

579 **Availability of data and materials**

580 The datasets generated during and/or analyzed during the current study are available from the
581 corresponding author on reasonable request.

582

583 **References**

584

- 585 1. Klemeš, J.J., et al., *Heat transfer enhancement, intensification and optimisation in heat*
586 *exchanger network retrofit and operation*. Renewable and Sustainable Energy Reviews,
587 2020. **120**: p. 109644.
- 588 2. Mohammed, H., et al., *Heat transfer and fluid flow characteristics in microchannels heat*
589 *exchanger using nanofluids: a review*. Renewable and Sustainable Energy Reviews, 2011.
590 **15**(3): p. 1502-1512.
- 591 3. Saidur, R., K. Leong, and H.A. Mohammed, *A review on applications and challenges of*
592 *nanofluids*. Renewable and sustainable energy reviews, 2011. **15**(3): p. 1646-1668.
- 593 4. Kumar, D.D. and A.V. Arasu, *A comprehensive review of preparation, characterization,*
594 *properties and stability of hybrid nanofluids*. Renewable and Sustainable Energy Reviews,
595 2018. **81**: p. 1669-1689.
- 596 5. Nazari, M.A., et al., *How to improve the thermal performance of pulsating heat pipes: a*
597 *review on working fluid*. Renewable and Sustainable Energy Reviews, 2018. **91**: p. 630-
598 638.
- 599 6. Choi, S.U. and J.A. Eastman, *Enhancing thermal conductivity of fluids with nanoparticles*.
600 1995, Argonne National Lab., IL (United States).
- 601 7. Kibria, M., et al., *A review on thermophysical properties of nanoparticle dispersed phase*
602 *change materials*. Energy Conversion and Management, 2015. **95**: p. 69-89.
- 603 8. Jama, M., et al., *Critical review on nanofluids: preparation, characterization, and*
604 *applications*. Journal of Nanomaterials, 2016. **2016**.
- 605 9. Sandhya, M., et al., *A systematic review on graphene-based nanofluids application in*
606 *renewable energy systems: Preparation, characterization, and thermophysical properties*.
607 Sustainable Energy Technologies and Assessments, 2021. **44**: p. 101058.

- 608 10. Leszczyńska, A., et al., *Polymer/montmorillonite nanocomposites with improved thermal*
609 *properties: Part I. Factors influencing thermal stability and mechanisms of thermal*
610 *stability improvement*. *Thermochimica acta*, 2007. **453**(2): p. 75-96.
- 611 11. Ibrahim, M., et al., *Comprehensive study concerned graphene nano-sheets dispersed in*
612 *ethylene glycol: Experimental study and theoretical prediction of thermal conductivity*.
613 *Powder Technology*, 2021. **386**: p. 51-59.
- 614 12. Abd Malek, M.N.F., et al., *Ultrasonication: a process intensification tool for methyl ester*
615 *synthesis: a mini review*. *Biomass Conversion and Biorefinery*, 2020: p. 1-11.
- 616 13. Ares, P. and K.S. Novoselov, *Recent advances in graphene and other 2D materials*. *Nano*
617 *Materials Science*, 2021.
- 618 14. Papanikolaou, I., et al., *Investigation of the dispersion of multi-layer graphene*
619 *nanoplatelets in cement composites using different superplasticiser treatments*.
620 *Construction and Building Materials*, 2021. **293**: p. 123543.
- 621 15. Sandhya, M., et al., *Ultrasonication an intensifying tool for preparation of stable*
622 *nanofluids and study the time influence on distinct properties of graphene nanofluids—A*
623 *systematic overview*. *Ultrasonics sonochemistry*, 2021. **73**.
- 624 16. Sundar, L.S., M.K. Singh, and A.C. Sousa, *Enhanced heat transfer and friction factor of*
625 *MWCNT–Fe₃O₄/water hybrid nanofluids*. *International Communications in Heat and*
626 *Mass Transfer*, 2014. **52**: p. 73-83.
- 627 17. Theres Baby, T. and R. Sundara, *Synthesis of silver nanoparticle decorated multiwalled*
628 *carbon nanotubes-graphene mixture and its heat transfer studies in nanofluid*. *AIP*
629 *Advances*, 2013. **3**(1): p. 012111.
- 630 18. Amiri, A., et al., *Highly dispersed multiwalled carbon nanotubes decorated with Ag*
631 *nanoparticles in water and experimental investigation of the thermophysical properties*.
632 *The Journal of Physical Chemistry C*, 2012. **116**(5): p. 3369-3375.
- 633 19. Watt, E., et al., *Hybrid biocomposites from polypropylene, sustainable biocarbon and*
634 *graphene nanoplatelets*. *Scientific reports*, 2020. **10**(1): p. 1-13.
- 635 20. Li, T., et al., *Developing fibrillated cellulose as a sustainable technological material*.
636 *Nature*, 2021. **590**(7844): p. 47-56.

- 637 21. Chirayil, C.J., L. Mathew, and S. Thomas, *REVIEW OF RECENT RESEARCH IN NANO*
638 *CELLULOSE PREPARATION FROM DIFFERENT LIGNOCELLULOSIC FIBERS.*
639 *Reviews on advanced materials science*, 2014. **37**.
- 640 22. Sandhya, M., et al. *Enhancement of the heat transfer in radiator with louvered fin by using*
641 *Graphene-based hybrid nanofluids.* in *IOP Conference Series: Materials Science and*
642 *Engineering*. 2021. IOP Publishing.
- 643 23. Sandhya, M., et al. *Enhancement of tribological behaviour and thermophysical properties*
644 *of engine oil lubricant by Graphene/Co-Cr nanoparticle additives for preparation of stable*
645 *nanolubricant.* in *IOP Conference Series: Materials Science and Engineering*. 2021. IOP
646 Publishing.
- 647 24. Hu, Z., et al., *Stable aqueous foams from cellulose nanocrystals and methyl cellulose.*
648 *Biomacromolecules*, 2016. **17**(12): p. 4095-4099.
- 649 25. Trache, D., V.K. Thakur, and R. Boukherroub, *Cellulose nanocrystals/graphene hybrids—*
650 *a promising new class of materials for advanced applications.* *Nanomaterials*, 2020. **10**(8):
651 p. 1523.
- 652 26. Sandhya, M., et al., *Experimental study on properties of hybrid stable & surfactant-free*
653 *nanofluids GNPs/CNCs (Graphene nanoplatelets/cellulose nanocrystal) in water/ethylene*
654 *glycol mixture for heat transfer application.* *Journal of Molecular Liquids*, 2022. **348**: p.
655 118019.
- 656 27. Yarmand, H., et al., *Study of synthesis, stability and thermo-physical properties of*
657 *graphene nanoplatelet/platinum hybrid nanofluid.* *International Communications in Heat*
658 *and Mass Transfer*, 2016. **77**: p. 15-21.
- 659 28. Kazemi, I., M. Sefid, and M. Afrand, *A novel comparative experimental study on*
660 *rheological behavior of mono & hybrid nanofluids concerned graphene and silica nano-*
661 *powders: Characterization, stability and viscosity measurements.* *Powder Technology*,
662 2020. **366**: p. 216-229.
- 663 29. Sarsam, W.S., et al., *Stability and thermophysical properties of non-covalently*
664 *functionalized graphene nanoplatelets nanofluids.* *Energy conversion and management*,
665 2016. **116**: p. 101-111.

- 666 30. Amiri, A., et al., *Backward-facing step heat transfer of the turbulent regime for*
667 *functionalized graphene nanoplatelets based water–ethylene glycol nanofluids.*
668 *International Journal of Heat and Mass Transfer*, 2016. **97**: p. 538-546.
- 669 31. Baby, T.T. and S. Ramaprabhu, *Enhanced convective heat transfer using graphene*
670 *dispersed nanofluids.* *Nanoscale research letters*, 2011. **6**(1): p. 289.
- 671 32. Cakmak, N.K., *The impact of surfactants on the stability and thermal conductivity of*
672 *graphene oxide de-ionized water nanofluids.* *Journal of Thermal Analysis and Calorimetry*,
673 2020. **139**(3): p. 1895-1902.
- 674 33. Kole, M. and T. Dey, *Investigation of thermal conductivity, viscosity, and electrical*
675 *conductivity of graphene based nanofluids.* *Journal of Applied Physics*, 2013. **113**(8): p.
676 084307.
- 677 34. Das, S., et al., *Role of graphene nanofluids on heat transfer enhancement in thermosyphon.*
678 *Journal of Science: Advanced Materials and Devices*, 2019. **4**(1): p. 163-169.
- 679 35. Sumanth, S., et al., *Effect of carboxyl graphene nanofluid on automobile radiator*
680 *performance.* *Heat Transfer—Asian Research*, 2018. **47**(4): p. 669-683.
- 681 36. Mehrali, M., et al., *Investigation of thermal conductivity and rheological properties of*
682 *nanofluids containing graphene nanoplatelets.* *Nanoscale research letters*, 2014. **9**(1): p.
683 15.
- 684 37. Yarmand, H., et al., *Graphene nanoplatelets–silver hybrid nanofluids for enhanced heat*
685 *transfer.* *Energy conversion and management*, 2015. **100**: p. 419-428.
- 686 38. Sarafraz, M., et al., *Thermal assessment of nano-particulate graphene-water/ethylene*
687 *glycol (WEG 60: 40) nano-suspension in a compact heat exchanger.* *Energies*, 2019.
688 **12**(10): p. 1929.
- 689 39. Akbari, A., et al., *Thermo-physical and stability properties of raw and functionalization of*
690 *graphene nanoplatelets-based aqueous nanofluids.* *Journal of Dispersion Science and*
691 *Technology*, 2019. **40**(1): p. 17-24.
- 692 40. Marcos, M.A., et al., *PEG 400-based phase change materials nano-enhanced with*
693 *functionalized graphene nanoplatelets.* *Nanomaterials*, 2018. **8**(1): p. 16.
- 694 41. Vallejo, J., et al., *Functionalized graphene nanoplatelet nanofluids based on a commercial*
695 *industrial antifreeze for the thermal performance enhancement of wind turbines.* *Applied*
696 *Thermal Engineering*, 2019. **152**: p. 113-125.

- 697 42. Said, Z., et al., *Thermophysical properties of water, water and ethylene glycol mixture-*
698 *based nanodiamond+ Fe₃O₄ hybrid nanofluids: An experimental assessment and*
699 *application of data-driven approaches.* Journal of Molecular Liquids, 2022. **347**: p.
700 117944.
- 701 43. Farhana, K., et al., *Experimental Studies on Thermo-Physical Properties of Nanocellulose-*
702 *Aqueous Ethylene Glycol Nanofluids.* Journal of Advanced Research in Materials Science,
703 2020. **69**(1): p. 1-15.
- 704 44. Ganeshkumar, J., et al., *Experimental study on density, thermal conductivity, specific heat,*
705 *and viscosity of water-ethylene glycol mixture dispersed with carbon nanotubes.* Thermal
706 Science, 2017. **21**(1 Part A): p. 255-265.
- 707 45. Wu, S. and O. Tahri, *State-of-art carbon and graphene family nanomaterials for asphalt*
708 *modification.* Road Materials and Pavement Design, 2021. **22**(4): p. 735-756.
- 709 46. Kulkarni, D.P., D.K. Das, and G.A. Chukwu, *Temperature dependent rheological property*
710 *of copper oxide nanoparticles suspension (nanofluid).* Journal of nanoscience and
711 nanotechnology, 2006. **6**(4): p. 1150-1154.
- 712 47. Sobczak, J., et al., *Thermophysical profile of ethylene glycol based nanofluids containing*
713 *two types of carbon black nanoparticles with different specific surface areas.* Journal of
714 Molecular Liquids, 2021. **326**: p. 115255.
- 715 48. Said, Z., et al., *Stability, thermophysical and electrical properties of synthesized carbon*
716 *nanofiber and reduced-graphene oxide-based nanofluids and their hybrid along with fuzzy*
717 *modeling approach.* Powder Technology, 2020. **364**: p. 795-809.
- 718 49. Vajjha, R., D. Das, and B. Mahagaonkar, *Density measurement of different nanofluids and*
719 *their comparison with theory.* Petroleum Science and Technology, 2009. **27**(6): p. 612-
720 624.
- 721 50. O'Neill, M., *Measurement of Specific Heat Functions by Differential Scanning Calorimetry.*
722 Analytical chemistry, 1966. **38**(10): p. 1331-1336.
- 723 51. Kodre, K., et al., *Differential scanning calorimetry: A review.* Research and Reviews:
724 Journal of Pharmaceutical Analysis, 2014. **3**(3): p. 11-22.
- 725 52. Su, W., et al., *Calibration of differential scanning calorimeter (DSC) for thermal*
726 *properties analysis of phase change material.* Journal of Thermal Analysis and
727 Calorimetry, 2021. **143**(4): p. 2995-3002.

- 728 53. Choi, T.J., et al., *Aqueous nanofluids containing paraffin-filled MWCNTs for improving*
729 *effective specific heat and extinction coefficient*. Energy, 2020. **210**: p. 118523.
- 730 54. Batakliiev, T., et al., *Effects of graphene nanoplatelets and multiwall carbon nanotubes on*
731 *the structure and mechanical properties of poly (lactic acid) composites: a comparative*
732 *study*. Applied Sciences, 2019. **9**(3): p. 469.
- 733 55. Rashad, M., et al., *Effect of graphene nanoplatelets (GNPs) addition on strength and*
734 *ductility of magnesium-titanium alloys*. Journal of Magnesium and alloys, 2013. **1**(3): p.
735 242-248.
- 736 56. Sandhya, M., et al., *Experimental study on properties of hybrid stable & surfactant-free*
737 *nanofluids GNPs/CNCs (Graphene nanoplatelets/cellulose nanocrystal) in water/ethylene*
738 *glycol mixture for heat transfer application*. Journal of Molecular Liquids, 2021: p.
739 118019.
- 740 57. Usri, N., et al., *Thermal conductivity enhancement of Al₂O₃ nanofluid in ethylene glycol*
741 *and water mixture*. Energy Procedia, 2015. **79**: p. 397-402.
- 742 58. Das, S.K., et al., *Temperature dependence of thermal conductivity enhancement for*
743 *nanofluids*. J. Heat Transfer, 2003. **125**(4): p. 567-574.
- 744 59. Amiri, A., et al., *Laminar convective heat transfer of hexylamine-treated MWCNTs-based*
745 *turbine oil nanofluid*. Energy conversion and management, 2015. **105**: p. 355-367.
- 746 60. Keblinski, P., et al., *Mechanisms of heat flow in suspensions of nano-sized particles*
747 *(nanofluids)*. International journal of heat and mass transfer, 2002. **45**(4): p. 855-863.
- 748 61. Sundar, L.S., et al., *Experimental investigation of the thermal transport properties of*
749 *graphene oxide/Co₃O₄ hybrid nanofluids*. International Communications in Heat and
750 Mass Transfer, 2017. **84**: p. 1-10.
- 751 62. Bing, N., et al., *3D graphene nanofluids with high photothermal conversion and thermal*
752 *transportation properties*. Sustainable Energy & Fuels, 2020. **4**(3): p. 1208-1215.
- 753 63. Ghozatloo, A., A. Rashidi, and M. Shariaty-Niassar, *Convective heat transfer enhancement*
754 *of graphene nanofluids in shell and tube heat exchanger*. Experimental Thermal and Fluid
755 Science, 2014. **53**: p. 136-141.
- 756 64. Selvam, C., D.M. Lal, and S. Harish, *Thermal conductivity enhancement of ethylene glycol*
757 *and water with graphene nanoplatelets*. Thermochemica Acta, 2016. **642**: p. 32-38.

- 758 65. Iranmanesh, S., et al., *Evaluation of viscosity and thermal conductivity of graphene*
759 *nanoplatelets nanofluids through a combined experimental–statistical approach using*
760 *respond surface methodology method*. International Communications in Heat and Mass
761 Transfer, 2016. **79**: p. 74-80.
- 762 66. Contreras, E.M.C., G.A. Oliveira, and E.P. Bandarra Filho, *Experimental analysis of the*
763 *thermohydraulic performance of graphene and silver nanofluids in automotive cooling*
764 *systems*. International Journal of Heat and Mass Transfer, 2019. **132**: p. 375-387.
- 765 67. Wang, Z., et al., *Experimental comparative evaluation of a graphene nanofluid coolant in*
766 *miniature plate heat exchanger*. International Journal of Thermal Sciences, 2018. **130**: p.
767 148-156.
- 768 68. Bakhtiari, R., et al., *Preparation of stable TiO₂-Graphene/Water hybrid nanofluids and*
769 *development of a new correlation for thermal conductivity*. Powder Technology, 2021.
770 **385**: p. 466-477.
- 771 69. Taherialekouhi, R., S. Rasouli, and A. Khosravi, *An experimental study on stability and*
772 *thermal conductivity of water-graphene oxide/aluminum oxide nanoparticles as a cooling*
773 *hybrid nanofluid*. International Journal of Heat and Mass Transfer, 2019. **145**: p. 118751.
- 774 70. Huminic, G., et al., *Study of the thermal conductivity of hybrid nanofluids: Recent research*
775 *and experimental study*. Powder Technology, 2020. **367**: p. 347-357.
- 776 71. Rostami, S., et al., *Modeling the thermal conductivity ratio of an antifreeze-based hybrid*
777 *nanofluid containing graphene oxide and copper oxide for using in thermal systems*.
778 Journal of Materials Research and Technology, 2021. **11**: p. 2294-2304.
- 779 72. Nguyen, C., et al., *Temperature and particle-size dependent viscosity data for water-based*
780 *nanofluids–hysteresis phenomenon*. International journal of heat and fluid flow, 2007.
781 **28**(6): p. 1492-1506.
- 782 73. Nguyen, C., et al., *Temperature and particle-size dependent viscosity data for water-based*
783 *nanofluids–hysteresis phenomenon*. International Journal of Heat and Fluid Flow, 2007.
784 **28**(6): p. 1492-1506.
- 785 74. Kishore, P., et al., *Preparation, characterization and thermo-physical properties of Cu-*
786 *graphene nanoplatelets hybrid nanofluids*. Materials Today: Proceedings, 2020. **27**: p. 610-
787 614.

- 788 75. Shahrul, I., et al., *A comparative review on the specific heat of nanofluids for energy*
789 *perspective*. Renewable and sustainable energy reviews, 2014. **38**: p. 88-98.
- 790 76. Adun, H., et al., *A critical review of specific heat capacity of hybrid nanofluids for thermal*
791 *energy applications*. Journal of Molecular Liquids, 2021. **340**: p. 116890.
- 792 77. Fazeli, I., M.R.S. Emami, and A. Rashidi, *Investigation and optimization of the behavior*
793 *of heat transfer and flow of MWCNT-CuO hybrid nanofluid in a brazed plate heat*
794 *exchanger using response surface methodology*. International Communications in Heat and
795 Mass Transfer, 2021. **122**: p. 105175.
- 796 78. Mousavi, S., F. Esmailzadeh, and X. Wang, *Effects of temperature and particles volume*
797 *concentration on the thermophysical properties and the rheological behavior of*
798 *CuO/MgO/TiO₂ aqueous ternary hybrid nanofluid*. Journal of Thermal Analysis and
799 Calorimetry, 2019. **137**(3): p. 879-901.
- 800 79. Minea, A.A., *Hybrid nanofluids based on Al₂O₃, TiO₂ and SiO₂: numerical evaluation of*
801 *different approaches*. International Journal of Heat and Mass Transfer, 2017. **104**: p. 852-
802 860.
- 803 80. Akilu, S., et al., *Properties of glycerol and ethylene glycol mixture based SiO₂-CuO/C*
804 *hybrid nanofluid for enhanced solar energy transport*. Solar Energy Materials and Solar
805 Cells, 2018. **179**: p. 118-128.
- 806 81. Gao, Y., et al., *Experimental investigation of specific heat of aqueous graphene oxide*
807 *Al₂O₃ hybrid nanofluid*. Thermal Science, 2021. **25**(1 Part B): p. 515-525.
- 808 82. Selvam, C., D. Mohan Lal, and S. Harish, *Thermal conductivity and specific heat capacity*
809 *of water–ethylene glycol mixture-based nanofluids with graphene nanoplatelets*. Journal
810 of Thermal Analysis and Calorimetry, 2017. **129**(2): p. 947-955.